

Topological Mott insulators of ultracold atomic mixtures induced by interactions in one-dimensional optical superlattices

Zhihao Xu¹ and Shu Chen^{1,*}

¹*Beijing National Laboratory for Condensed Matter Physics,
Institute of Physics, Chinese Academy of Sciences, Beijing 100190, China*

(Dated: October 21, 2018)

We present exactly solvable examples that topological Mott insulators can emerge from topologically trivial states due to strong interactions between atoms for atomic mixtures trapped in one-dimensional optical superlattice systems. The topological Mott insulating state is characterized by nonzero Chern number and appears in the strongly interacting limit as long as the total band filling factor is an integer, which is not sensitive to the filling of each component. The topological nature of the Mott phase can be revealed by observing the density profile of the trapped system. Our results can be also generalized to the multi-component atomic systems.

PACS numbers: 05.30.Fk, 03.75.Hh, 73.21.Cd, 67.85.Pq

I. INTRODUCTION

Topological band insulators have attracted great attention in condensed matter physics since they were discovered in spin-orbit coupled two- and three-dimensional systems^{1,2}. As the topological insulator (TI) is expected to be robust against weak perturbations, it is important to consider the effect of interactions on the topological band insulators³⁻⁶. Although generally a strong interaction may open the energy gap and break the TI, there exists a class of topological insulator called as the topological Mott insulator (TMI), where the interaction effects are responsible for TI behavior⁷. The topological Mott phases have attracted increasing attention⁸⁻¹⁵ since the concept is proposed as interaction plays a crucial role in the formation of both the Mott phase and nontrivial topology. As almost all these results based on the mean-field approximation, examples with the interaction effect counted exactly is particularly important for our understanding of the TMI.

In this work, we explore the realization of topological Mott phases in cold atomic systems trapped in one-dimensional (1D) quasi-periodic optical lattices, which can be generated by superimposing two 1D optical lattices with commensurate or incommensurate wavelengths¹⁶⁻¹⁸. Cold atomic systems in 1D quasi-periodic lattices have been extensively studied¹⁹⁻²² with a focus on the Anderson localization¹⁷. However, their nontrivial topological features are recognized only very recently^{23,24}. Particularly, with the experimental observation of the topological edge states in 1D photonic quasicrystals²⁴ there is a growing interest in the study of topological properties in the 1D quasi-periodic lattices²⁵⁻³⁰. It has been shown that the free fermion system with its sub-bands being fully filled is a topological nontrivial insulator characterized by a nonzero Chern number in a two-dimensional (2D) parameter space²³. In this work, we study the interacting atomic mixtures in the 1D superlattice with its sub-bands are partially filled by atoms. In the absence of inter-component interaction, the system

may be a Fermi metal, a Bose superfluid or their mixture, depending on the component of mixture being fermion or boson. We find that a TMI may emerge in the strongly interacting regime if the total band filling is an integer. This conclusion is exact in the limit of infinitely strong interaction (ISI) as it is based on an exact mapping which relates the many-body wavefunction of two-component mixture to the wavefunction of free fermion system. Our study provides a simple way to realize the TMI in cold atomic systems and may deepen our understanding of the TMI.

II. MODELS AND RESULTS

A. Models of interacting atomic mixtures in optical superlattices

We consider the 1D atomic mixtures loaded in a bichromatic optical lattice¹⁶⁻¹⁸, which is described by $H = H_0 + H_I$ with

$$H_0 = -t \sum_{i,\sigma=\uparrow,\downarrow} (\hat{c}_{i,\sigma}^\dagger \hat{c}_{i+1,\sigma} + \text{H.c.}) + \sum_{i,\sigma=\uparrow,\downarrow} V_i \hat{n}_{i,\sigma} \quad (1)$$

and

$$H_I = U \sum_i \hat{n}_{i,\uparrow} \hat{n}_{i,\downarrow} + \sum_i \frac{1}{2} U_\sigma \hat{n}_{i,\sigma} (\hat{n}_{i,\sigma} - 1), \quad (2)$$

where $V_i = \lambda \cos(2\pi\alpha i + \delta)$ with λ controlling the strength of commensurate potential, α tuning the modulation period and δ being an arbitrary phase, $c_{i,\sigma}$ are bosonic or fermionic annihilation operators localized on site i , and $n_{i\sigma} = c_{i\sigma}^\dagger c_{i\sigma}$. Here $\sigma = \uparrow, \downarrow$ denotes the pseudo-spin index of two components of atomic mixtures, which can be either fermion or boson. For the two-component systems, there are three kinds of mixtures, i.e., Fermi-Fermi (FF) mixture, Bose-Bose (BB) mixture and Fermi-Bose (FB) mixture. The interaction parameter U denotes the inter-component interaction strength, and U_σ the intra-component interaction strength with $U_\sigma = 0$ between

fermionic atoms. Both U and U_σ can be experimentally tuned to the limit of ISI by the Feshbach resonance³¹. The hopping amplitude t is set to be the energy unit ($t = 1$).

In the absence of interactions, the eigenvalue equation, namely the Harper equation, is given by

$$-[\phi_n(i+1) + \phi_n(i-1)] + \lambda \cos(2\pi\alpha i + \delta)\phi_n(i) = \epsilon_n \phi_n(i), \quad (3)$$

where $\phi_n(i)$ denotes the single particle wave function and ϵ_n the n -th single particle eigenenergy^{32–34}. For a superlattice with $\alpha = p/q$ (p and q are co-prime integers), the system has a unit cell of q sites and the single-particle spectrum is split into q bands. Given that the number of σ -component atoms is N_σ and the number of lattice sites is L , we define the component-depending band filling factor as $\nu_\sigma = N_\sigma/N_{cell}$ with $N_{cell} = L/q$ being the number of primitive cells. For a Fermi system, the system with the band filling factor $\nu_\sigma = m$ (m is an integer smaller than q) corresponds to a band insulator with the lowest m bands being fully filled by the σ -component fermion. Such a band insulator has been demonstrated to be characterized by a nontrivial topological Chern number in a 2D parameter space spanned by momentum and the phase of δ ²³. In this work we shall consider the two-component system with fractional filling factors ν_\uparrow and ν_\downarrow but the total band filling factor $\nu = \nu_\uparrow + \nu_\downarrow$ being an integer. For the noninteracting system, the sub-band is only partially filled and the system is a topologically trivial conductor. We shall show that a Mott phase can emerge from the conducting phase with an integer total filling factor when the interaction effect is considered.

B. Emergence of Mott phase

To give a concrete example, we first consider the FF mixture described by the Hamiltonian (1) and (2) with $U_\sigma = 0$. We consider the case with $\alpha = 1/3$ and $\nu = 1$, for which $n = N/L = 1/3$, and calculate the charge gap defined as $\Delta = [E_0(N+1) + E_0(N-1)]/2 - E_0(N)$ by numerically diagonalizing the Hamiltonian, where $E_0(N)$ represent the ground state (GS) energy for the N -atom system. In the Fig.1a, we show the charge gap versus U for the equal-mixing case with $\nu_\uparrow = \nu_\downarrow = 1/2$. For the system with either $N = 4$ or $N = 6$, the charge gap increases with increasing U and tends to $\Delta_b/2$ in the large U limit, where Δ_b represents the band gap between the lowest band and the second one. The numerical results indicate that a Mott insulator is emergent in the strongly interacting limit as the gap is induced by the interaction.

Next we calculate the charge gap versus U for various U' for the equal-mixing FB mixture. Here we use U' to represent intra-component bosonic interaction strength for the two-component FB mixture. As shown in Fig.1b for the system of $N = 4$, with increasing U' , the charge gap increases and the curve approaches the curve of FF mixture. In the limit of hard-core boson, i.e., $U_\sigma \rightarrow \infty$

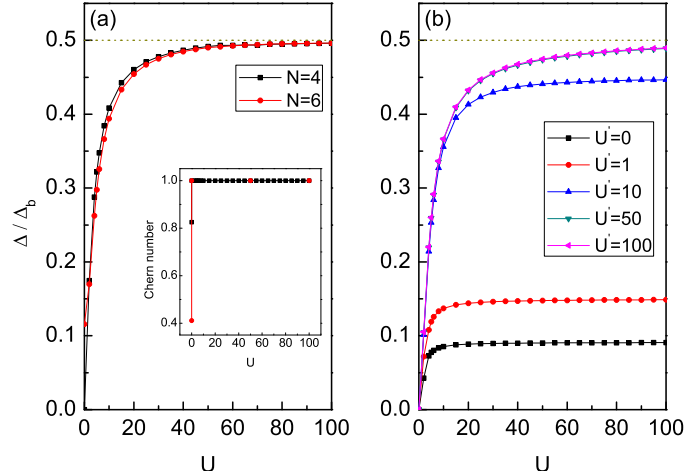


FIG. 1: (Color online) The charge gap versus the interaction strength U for equal-mixing Fermi-Fermi system (a) and Fermi-Bose system (b) with $\alpha = 1/3$, $\lambda = 1.5$, $\delta = 0$, and $n = 1/3$ under periodic boundary conditions (PBC). The inset in (a) shows the Chern number versus U .

for the BB mixture and $U' \rightarrow \infty$ for the FB mixture, both the BB and FB model can be mapped into the Fermi Hubbard model by extended Jordan-Wigner transformations³⁵. Therefore, the above discussion on the FF mixture can be directly applied to hard-core-boson limit of the FB and BB mixtures.

C. Atomic mixtures in the strongly interacting limit

The emergence of the charge gap for the superlattice system with integer band filling factor can be clearly understood in the limit of ISI, where we can construct the many-body wavefunction of the FF system exactly by using the hard-core contact boundary condition (HCCBC)³⁶ and group theoretical methods³⁷. Combining with the Pauli exclusion principle, the effect of an ISI can be reduced to the HCCBC $\Psi(x_1, \sigma_1; \dots; x_N, \sigma_N) |_{x_i=x_j} = 0$, which does not depend on spin configurations. According to Ref.³⁷, the many-body wave function can be represented as $\Psi = \Psi_A \Psi_S$, where the spatial wave function Ψ_A is composed of Slater determinant of $N = N_\uparrow + N_\downarrow$ orbitals $\phi_1(x), \dots, \phi_N(x)$, given by

$$\psi_A(x_1, \dots, x_N) = (N!)^{-\frac{1}{2}} \det[\phi_n(x_i)]_{i=1, \dots, N}^{n=1, \dots, N} \quad (4)$$

with $\phi_n(x)$ ($x = ia$ with a the lattice constant) the eigenstate of the single particle Hamiltonian H_0 , whereas Ψ_S is a mapping function composed of linear combination of production of sign function and basis tensor of spin, whose explicit form is given in Ref.³⁷. Effectively, the

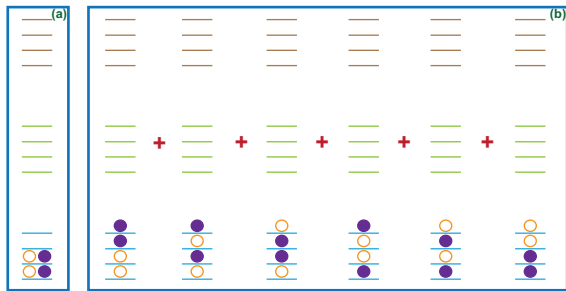


FIG. 2: (Color online) Schematic diagram for the ground state energy level occupations for system with $\alpha = 1/3$, $N_{\uparrow} = N_{\downarrow} = 2$ and $L = 12$. (a) is for $U = 0$ and (b) is for $U \rightarrow \infty$.

effect of infinite repulsion is to generate a Pauli exclusion between different components of fermions, which has been experimentally observed in a two-particle system of fermionic ${}^6\text{Li}$ atoms with tunable interactions³⁸.

Now we can understand the formation of Mott phase by considering the case in the limit of ISI. As illustrated in Fig.2, for the superlattice with $\alpha = 1/3$, the energy levels split into three bands. When $U = 0$, the lowest band is only partially filled for $\nu_{\uparrow} = \nu_{\downarrow} = 1/2$. However the lowest band is fully filled in the limit of $U \rightarrow \infty$ corresponding to $\nu = 1$ as each energy level can only be occupied by a fermion with either spin up or spin down, and consequently a charge gap is opened. According to the definition of charge gap, we have $\Delta = \Delta_b/2$ as adding a fermion costs the energy of Δ_b , which is consistent with the numerical result displayed in Fig.1. For a general case with $\alpha = 1/q$, the energy levels are composed of q bands. As long as $\nu = m$ with $m = 1, \dots, q-1$, a Mott insulator is formed as $U \rightarrow \infty$. For a fractional ν , for example, $\nu < 1$, the lowest band is not fully filled even in the limit of ISI, and thus no finite charge gap is opened.

The above discussion can be directly applied to the BB mixture and FB mixture in the limit of ISI. As $U \rightarrow \infty$ and $U_{\sigma} \rightarrow \infty$, the effect of ISIs can be also reduced to the HCCBC, which enforces an effective Pauli exclusion to hard-core bosons and between different components of atoms. Consequently, the exact wave function of the system can be also represented as $\Psi = \Psi_A \Psi_S$, where Ψ_A is identical to the expression of (4), but Ψ_S has different form for different kind of mixtures^{36,37,39}. For the BB mixture, $\Psi_S = \prod_{1 \leq i, j \leq N} \text{sgn}(x_i - x_j)$, where $\text{sgn}(x)$ is the sign function. The explicit form of the mapping function Ψ_S for the FB mixture is given in Ref.³⁶.

D. Topological feature of the Mott phase

To characterize the topological feature of the many-body states, it is convenient to introduce a generalized boundary phase θ by applying the twist boundary condition (TBC). In the 2D parameter space of (θ, δ) , we can calculate the Chern number of the many-body state, which is defined as an integral invariant

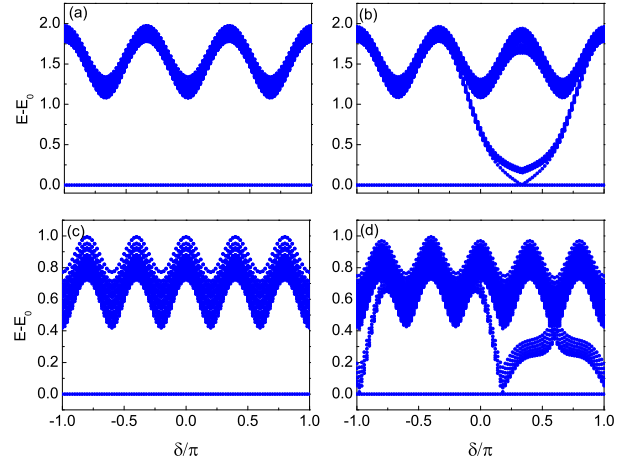


FIG. 3: (Color online) Low-energy spectrum versus δ for two-component mixture systems with $\lambda = 1.5$ and different α in the infinitely repulsive limit. (a) $\alpha = 1/3$, $N = 30$, $L = 90$ under PBC; (b) $\alpha = 1/3$, $N = 30$, $L = 91$ under OBC; (c) $\alpha = 1/5$, $N = 40$, $L = 100$ under PBC; (d) $\alpha = 1/5$, $N = 40$, $L = 101$ under OBC.

$C = \frac{1}{2\pi} \int d\theta d\delta F(\theta, \delta)$, where $F(\theta, \delta) = \text{Im}(\langle \frac{\partial \Psi}{\partial \delta} | \frac{\partial \Psi}{\partial \theta} \rangle - \langle \frac{\partial \Psi}{\partial \theta} | \frac{\partial \Psi}{\partial \delta} \rangle)$ is the Berry curvature^{40,41}. For the two-component mixtures in the limit of ISI, we notice that the many-body wave functions under TBC can be represented as $\Psi(\theta, \delta) = \Psi_A(\theta, \delta) \Psi_S$, where only Ψ_A varies with the change of θ and δ , whereas Ψ_S is independent of θ and δ as it is composed of combination of production of sign functions. This greatly simplifies the calculation of the Chern number as $F(\theta, \delta) = \text{Im}(\langle \frac{\partial \Psi_A}{\partial \delta} | \frac{\partial \Psi_A}{\partial \theta} \rangle - \langle \frac{\partial \Psi_A}{\partial \theta} | \frac{\partial \Psi_A}{\partial \delta} \rangle)$, where Ψ_A is given by Eq.(4). Consequently, the Chern number for atomic mixtures composed of N_{\uparrow} and N_{\downarrow} two-component atoms is identical to the Chern number of the system composed of N free fermions. For the system with $\alpha = 1/3$, the Mott insulators are formed when $\nu = 1$ and $\nu = 2$, corresponding to states with Chern number $C = 1$ and $C = -1$, which characterizes the Mott insulators being topologically nontrivial. For the system with a finite U , the Chern number can be obtained via numerically calculating the many-body wavefunction under TBC⁴¹. As shown in the inset of Fig.1a, the Chern number for systems with $\nu = 1$ approaches 1 even for a very small U . Such a result reminds us a similar phenomenon in the 1D Hubbard model without periodic modulation, for which the half-filling Hubbard system enters the Mott phase for an arbitrary repulsive interaction as shown in the seminal work of Lieb and Wu⁴². The results for finite U indicate that our exact conclusions in the limit of ISI are robust even when the interaction deviates the limit of ISI. When the filling deviates $\nu = 1$, the Chern number is no longer an integer number.

According to the bulk-edge correspondence in general

topological insulators, one may expect that the TMIs should display nontrivial edge states for the system with open boundary conditions (OBC). To see it clearly, we display the excitation spectrum versus the phase δ for mixture systems in the strongly interacting limit with $\nu = 1$, $\alpha = 1/3$ and $\nu = 2$, $\alpha = 1/5$ in Fig.3. The system with $\nu = 1$ and $\alpha = 1/3$ is a TMI characterized by the Chern number $C = 1$, whereas the TMI corresponding to $\nu = 2$ and $\alpha = 1/5$ is characterized by $C = 2$. As shown in Fig. 3a and Fig. 3c, there is an obvious gap between the GS and the first excited state for systems with PBC. However, as shown in Fig. 3b and Fig. 3d, edge states appear in the gap regimes for systems with OBC. As the phase varies from $-\pi$ to π , the edge states connect the GS to the excited band.

For the periodic modulation system under PBC considered in the current work, the unit cell is composed of q different sites, and one need take the lattice size L as $L = qN_{cell}$ to fulfill the PBC. However, for the system under OBC, one can take the lattice size $L = qN_{cell} + i$ with $i = 0, \dots, q - 1$, i.e., we have q different choices⁴³. For example, for the periodic system with $\alpha = 1/3$ and $L = 90$, we should have three different choices of lattice sizes with $L = 90, 91$, and 92 under OBC. In Fig. 3b, we only present the example with $L = 91$. To see clearly the effect of lattice sizes, here we present the energy spectrums versus δ with different lattice sizes under OBC in Fig.4. The top three figures in Fig.4 are for single-particle spectra and the bottom ones are for many-body systems with $N = 30$ in the strongly repulsive limit. Three columns from left to right are with $L = 90, 91$ and 92 , respectively. As shown in the figure, the positions of the gap-less single-particle edge modes change with the change of lattice sizes, and correspondingly shapes of many-body edge modes also change. However, the edge modes always connect ground state and excited bands in the bulk gap regime for different sizes. It is clear that the choice of different lattice sizes under OBC affects the concrete shape of edge modes, but does not change its topological properties demonstrating by edge modes connecting ground state and excited bands in the band gap regime of the corresponding bulk system.

When the interaction deviates from the limit of ISI, despite of the exact mapping no longer holding true, our numerical results indicate that the topological Mott phase still exists. To see how the edge states change when U deviates the limit of ISI, we display the excitation spectrum versus the phase δ for the FF mixture system with $\alpha = 1/3$, $N_{\uparrow} = N_{\downarrow} = 2$, $L = 12$ and various U under the OBC in Fig.5. As shown in Fig.5, the excitation spectrum for the system with $U = 100$ exhibits almost the same behavior of system in the limit of ISI as shown in Fig.4b. For $U = 10$ and $U = 5$, the spectra still have similar structures but with the GS levels being broadened for smaller U due to spin fluctuations as the degeneracy of GSs in the limit of ISI is lifted for finite interactions. However, for $U = 1$, no obvious edge modes can be detected as no an obvious gap regime appears in the weakly

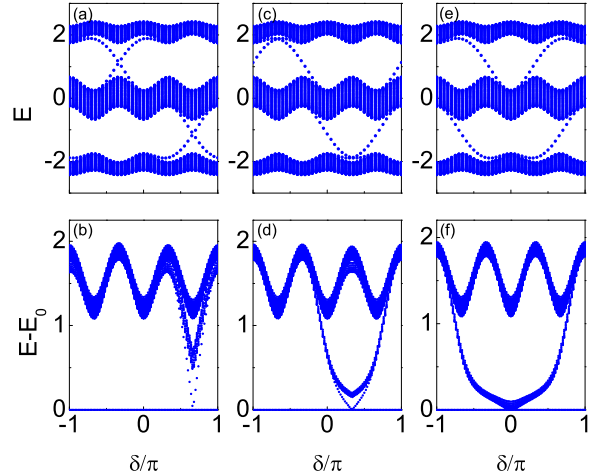


FIG. 4: (Color online) Low-energy spectrum versus δ for the systems with $\lambda = 1.5$, $\alpha = 1/3$, and various L under open boundary condition. The top three figures are for single-particle spectrums and the bottom ones are for many-body systems with $N = 30$ in the strongly repulsive limit. Three columns from left to right are with $L = 90, 91$ and 92 , respectively.

interacting regime even under the PBC. In order to see the effect of lattice size, we also present results for the system with $\alpha = 1/3$, $N_{\uparrow} = N_{\downarrow} = 2$ and a different lattice size of $L = 13$ in Fig.6. It is clear that the low-energy excitation spectra have similar behaviors as that of the system with $L = 12$ shown in Fig.5. For both systems, the edge modes connect the lower energy parts and the higher excited ones, which is consistent with the results in the limit of ISI as shown in Fig.4(b) and Fig.4(d).

Our results can be directly extended to the general multi-component atomic systems trapped in 1D superlattices. When the inter-specie and inner-specie interactions between atoms go to the strongly interacting limit, an effective Pauli exclusion between atoms arises. Therefore, a TMI is expected to appear in the topologically nontrivial superlattice as long as the total filling factor $\nu = \sum_{\kappa} \nu_{\kappa}$ is an integer, where κ is the component index of the multi-component atomic mixture.

E. Experimental detection

A possible way to observe the TMI is to detect the density distribution of the superlattice systems with an external confining potential, i.e., V_i in Eq.(1) is replaced by $V_i = \lambda \cos(2\pi\alpha i + \delta) + V_H(i - i_0)^2$, where V_H is the strength of the harmonic trap with i_0 being the position of trap center. In Fig.7, we show the local average density distribution of two-component fermions with imbalance populations trapped in the optical superlattice with a harmonic trap. The local average density is defines

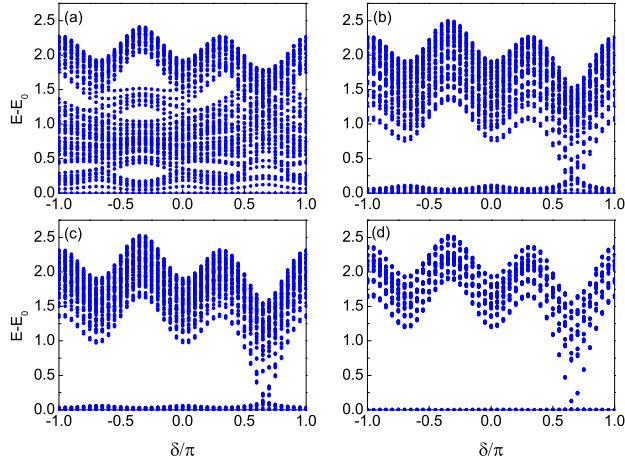


FIG. 5: (Color online) Low-energy spectrum versus δ for the Fermi-Fermi mixture with $\alpha = 1/3$, $\lambda = 1.5$, $N_{\uparrow} = N_{\downarrow} = 2$, $L = 12$ and various U under open boundary condition. (a) $U = 1$, (b) $U = 5$, (c) $U = 10$ and (d) $U = 100$.

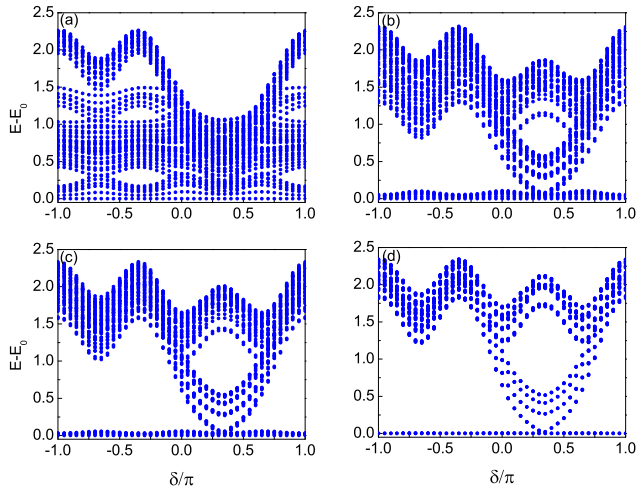


FIG. 6: (Color online) Low-energy spectrum versus δ for the Fermi-Fermi mixture with $\alpha = 1/3$, $\lambda = 1.5$, $N_{\uparrow} = N_{\downarrow} = 2$, $L = 13$ and various U under OBC. (a) $U = 1$, (b) $U = 5$, (c) $U = 10$ and (d) $U = 100$.

as $\rho_i = \sum_{j=-M}^M n_{i+j}/(2M+1)$ with $M \ll L^{23}$, where $n_i = \langle \hat{n}_{i,\uparrow} \rangle + \langle \hat{n}_{i,\downarrow} \rangle$. In the strongly interacting limit, two plateaus with $\rho = 1/3$ and $\rho = 2/3$ appear for $\alpha = 1/3$, whereas four plateaus with $\rho = 1/5, 2/5, 3/5, 4/5$ appear for $\alpha = 1/5$. We note that locations of plateaus appear at $\rho(\alpha) = \alpha, 1 - \alpha, 2\alpha, 1 - 2\alpha, \dots$, if the values are in the range of $(0, 1)$. For contrast, the density profiles for $U = 0$ do not exhibit these plateaus. The Chern number can thus be deduced from the plateau distribution by using the Streda formula^{23,44} $C = \frac{\partial \rho(\alpha)}{\partial \alpha}$. It is straight-

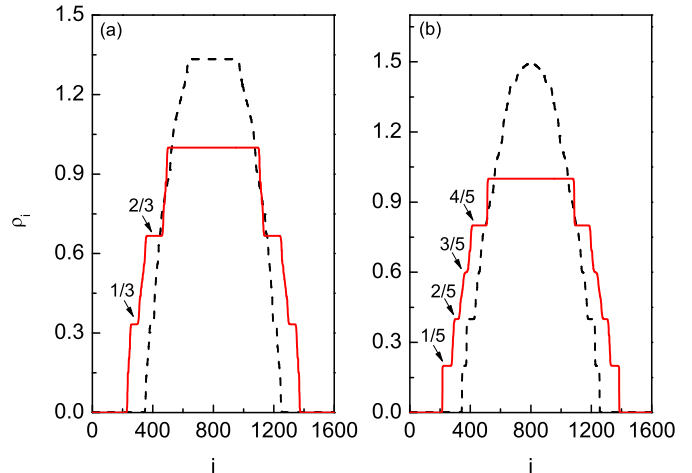


FIG. 7: (Color online) The local average density distributions for the superlattice with $\alpha = 1/3$ (a), and $\alpha = 1/5$ (b) trapped in the harmonic trap. The system is with 1600 sites, $N_{\uparrow} = 400$, $N_{\downarrow} = 500$, $\lambda = 1.5$, $\delta = 0$ and $V_H = 2 \times 10^{-6}$. The dash line is for the case of $U = 0$ and the solid line is for the case of $U \rightarrow \infty$. Here, we take $M = (q - 1)/2$.

forward to get $C = 1, -1$ for $\rho_i = \alpha, 1 - \alpha$ and $C = 2, -2$ for $\rho_i = 2\alpha, 1 - 2\alpha$. Alternative methods of detecting Chern numbers in optical lattices through time-of-flight images have also been proposed^{45,46}.

III. SUMMARY

In summary, we studied the realization of TMIs in interacting atomic mixtures trapped in 1D optical superlattices. We give a clear interpretation for the formation of TMI by using an exact mapping, which relates the many-body wavefunction of atomic mixtures in the strongly interacting limit to that of the free fermion system. The TMI displays nontrivial edge states and can be characterized by a nonzero Chern number. The topological feature of the Mott insulator can be revealed by detecting plateaus of density profiles of the trapped lattice systems. Our results pave the way for experimentally studying TMIs in 1D optical lattices and can be directly extended to the general multi-component atomic systems trapped in 1D superlattices.

Acknowledgments

We thank L.-J. Lang for helpful discussions. This work has been supported by National Program for Basic Research of MOST, NSF of China under Grants No.11121063 and No.11174360, and 973 grant.

Appendix A

In the appendix, we make a comparison between the interacting Fermi-Fermi mixtures described by Hamiltonian (1) and (2) and the interacting Hofstadter model described by $H^{2D} = H_0^{2D} + H_I^{2D}$ ³³. For a two-dimensional square lattice in a uniform perpendicular magnetic field B , under the Landau gauge $\vec{A} = B(0, x, 0)$, the noninteracting part H_0^{2D} is given by³²

$$H_0^{2D} = \sum_{i,j,\sigma=\uparrow,\downarrow} -t_x \hat{c}_{i,j,\sigma}^\dagger \hat{c}_{i+1,j,\sigma} - t_y e^{-i2\pi\alpha i} \hat{c}_{i,j,\sigma}^\dagger \hat{c}_{i,j+1,\sigma} + \text{H.c.}, \quad (\text{A1})$$

where t_x and t_y are the strength of the nearest-neighbor hopping along the x and y directions, $\hat{c}_{i,j,\sigma}$ is the annihilation operator of the fermions with spin σ at (i, j) in the lattice, and α is the ratio of flux through a unit cell to one flux quantum. For a Fermi-Fermi mixture, the on-site term at (i, j) site in the lattices is given by

$$H_I^{2D} = U \sum_{i,j} \hat{n}_{i,j,\uparrow} \hat{n}_{i,j,\downarrow}, \quad (\text{A2})$$

Taking a Fourier transformation in the y direction $\hat{c}_{i,j,\sigma} = \frac{1}{\sqrt{L_{k_y}}} \sum_{k_y} e^{-ik_y j} \hat{c}_{i,k_y,\sigma}$, we can rewrite the Hamiltonian $H^{2D} = H_0^{2D} + H_I^{2D}$ in the k_y -momentum space as

$$H_0^{2D} = \sum_{i,k_y,\sigma=\uparrow,\downarrow} -t_x \left(\hat{c}_{i,k_y,\sigma}^\dagger \hat{c}_{i+1,k_y,\sigma} + \text{H.c.} \right) - 2t_y \cos(2\pi\alpha i + k_y) \hat{n}_{i,k_y,\sigma} \quad (\text{A3})$$

and

$$H_I^{2D} = \frac{U}{L_y} \sum_i \sum_{k_{y1}, k_{y2}, k_{y3}, k_{y4}} \delta_{k_{y1} - k_{y2} + k_{y3} - k_{y4}, 2\pi} \hat{c}_{i,k_{y1},\uparrow}^\dagger \hat{c}_{i,k_{y3},\downarrow}^\dagger \hat{c}_{i,k_{y4},\downarrow} \hat{c}_{i,k_{y2},\uparrow}, \quad (\text{A4})$$

In the limit of $U \rightarrow 0$, by making substitutions of $t_x \rightarrow t$, $-2t_y \rightarrow \lambda$, and $k_y \rightarrow \delta$, the Hamiltonian H^{2D} can be mapped to the one-dimensional model with a periodic or quasi-periodic modulation (Hamiltonian (1) in the main text) which depends on α being rational or irrational number. In spite of the existence of such a mapping for the noninteracting systems, the interacting term H_I^{2D} under the Fourier transformation displays obvious different form as the on-site term of the Hamiltonian (2) in the main text. While the interacting term for the 1D model is only relevant to a given parameter of δ , the interacting term H_I^{2D} couples different k_y modes (corresponding to δ) together. Therefore, the exact results for the one-dimensional systems in the strongly interacting limit can not be applied to the corresponding two-dimensional interacting Hofstadter model directly.

-
- * Electronic address: schen@aphy.iphy.ac.cn
- ¹ M. Z. Hasan and C. L. Kane, Rev. Mod. Phys. **82**, 3045 (2010).
 - ² X.-L. Qi and S.-C. Zhang, Rev. Mod. Phys. **83**, 1057 (2011).
 - ³ M. Dzero, K. Sun, V. Galitski, and P. Coleman, Phys. Rev. Lett. **104**, 106408 (2010).
 - ⁴ Z. Wang, X.-L. Qi, and S.-C. Zhang Phys. Rev. Lett. **105**, 256803 (2010); L. Wang, X. Dai, and X. C. Xie, Phys. Rev. B **84**, 205116 (2011).
 - ⁵ S.-L. Yu, X. C. Xie, and J.-X. Li, Phys. Rev. Lett. **107**, 010401 (2011).
 - ⁶ H. M. Guo and S.-Q. Shen Phys. Rev. B **84**, 195107 (2011).
 - ⁷ S. Raghu, X.-L. Qi, C. Honerkamp, and S.-C. Zhang, Phys. Rev. Lett. **100**, 156401 (2008).
 - ⁸ D. A. Pesin and L. Balents, Nature Physics **6**, 376 (2010).
 - ⁹ Y. Zhang, Y. Ran, and A. Vishwanath, Phys. Rev. B **79**, 245331 (2009); S. Rachel and K. Le Hur, Phys. Rev. B **82**, 075106 (2010).
 - ¹⁰ X. Zhang, H. Zhang, J. Wang, C. Felser, S.-C. Zhang, Science **335**, 1464 (2012).
 - ¹¹ K. Sun, H. Yao, E. Fradkin, S. A. Kivelson, Phys. Rev. Lett. **103**, 046811 (2009); M. Hohenadler, T. C. Lang, and F. F. Assaad, Phys. Rev. Lett. **106**, 100403 (2011); J. Wen, A. Rüegg, C. C. J. Wang, and G. A. Fiete, Phys. Rev. B **82**, 075125 (2010); C. N. Varney, K. Sun, M. Rigol, and V. Galitski, Phys. Rev. B **82**, 115125 (2010).
 - ¹² D. Zheng, G. M. Zhang, and C. Wu, Phys. Rev. B **84**, 205121 (2011); S. Uebelacker and C. Honerkamp, Phys. Rev. B **84**, 205122 (2011); J. Wen, M. Kargarian, A. Vaezi, and G. A. Fiete, Phys. Rev. B **84**, 235149 (2011); C. N. Varney, K. Sun, M. Rigol, and V. Galitski, Phys. Rev. B **84**, 241105(R) (2011).
 - ¹³ C. Griset and C. Xu, Phys. Rev. B **85**, 045123 (2012); Y. Tada, R. Peters, M. Oshikawa, A. Koga, N. Kawakami, and S. Fujimoto, Phys. Rev. B **85**, 165138 (2012); A. Vaezi, M. Mashkooi, and M. Hosseini, Phys. Rev. B **85**, 195126 (2012).
 - ¹⁴ W. Wu, S. Rachel, W. M. Liu, and K. L. Hur, Phys. Rev. B **85**, 205102 (2012); L. Wang, X. Dai and X. C. Xie, EPL **98**, 57001 (2012); A. Dauphin, M. Müller, M. A. Martin-Delgado, Phys. Rev. A **86**, 053618 (2012).
 - ¹⁵ M. Hohenadler, F. F. Assaad, J. Phys.: Condens. Matter **25**, 143201 (2013); J. Werner and F. F. Assaad arXiv:1302.1874.
 - ¹⁶ L. Fallani, J. E. Lye, V. Guarrera, C. Fort, and M. Inguscio, Phys. Rev. Lett. **98**, 130404 (2007).
 - ¹⁷ G. Roati *et al.*, Nature (London) **453**, 895 (2008).

- ¹⁸ B. Deissler *et al.*, Nat. Phys. **6**, 354 (2010).
- ¹⁹ T. Roscilde, Phys. Rev. A **77**, 063605 (2008).
- ²⁰ G. Roux, T. Barthel, I. P. McCulloch, C. Kollath, U. Schollwöck, and T. Giamarchi, Phys. Rev. A **78**, 023628 (2008); X. Deng, R. Citro, A. Minguzzi, and E. Orignac, Phys. Rev. A **78**, 013625 (2008).
- ²¹ T. Yamashita, N. Kawakami, and M. Yamashita, Phys. Rev. A **74**, 063624 (2006).
- ²² X. Cai, S. Chen, and Y. Wang, Phys. Rev. A **81**, 023626 (2010); Phys. Rev. A **81**, 053629 (2010).
- ²³ L.-J. Lang, X. M. Cai, and S. Chen, Phys. Rev. Lett. **108**, 220401 (2012).
- ²⁴ Y. E. Kraus, Y. Lahini, Z. Ringel, M. Verbin, and O. Zeitlinger, Phys. Rev. Lett. **109**, 106402 (2012).
- ²⁵ F. Mei, S.-L. Zhu, Z.-M. Zhang, C. H. Oh, and N. Goldman, Phys. Rev. A **85**, 013638 (2012); S.-L. Zhu, Z. D. Wang, Y. -H. Chan, and L. -M. Duan, Phys. Rev. Lett. **110**, 075303 (2013).
- ²⁶ Y. E. Kraus and O. Zeitlinger, Phys. Rev. Lett. **109**, 116404 (2012); M. Verbin, Y. E. Kraus, O. Zeitlinger, Y. Lahini, and Y. Silberberg, Phys. Rev. Lett. **110**, 076403 (2013).
- ²⁷ Z. H. Xu, L. H. Li, and S. Chen, Phys. Rev. Lett. **110**, 215301 (2013).
- ²⁸ M. Tezuka and N. Kawakami, Phys. Rev. B **85**, 140508 (2012).
- ²⁹ O. Viyuela, A. Rivas, and M. A. Martin-Delgado, Phys. Rev. B **86**, 155140 (2012).
- ³⁰ L.-J. Lang, and S. Chen, Phys. Rev. B **86**, 205135 (2012); X. Cai, L.-J. Lang, S. Chen, and Y. Wang, Phys. Rev. Lett. **110**, 176403 (2013); W. DeGottardi, D. Sen, and S. Vishveshwara, Phys. Rev. Lett. **110**, 146404 (2013); I. I. Satija and G. G. Naumis, arXiv:1210.5159.
- ³¹ S. Inouye, M. R. Andrews, J. Stenger, H.-J. Miesner, D. M. Stamper-Kurn and W. Ketterle, Nature **392**, 151 (1998); C. Chin, R. Grimm, P. Julienne, E. Tiesinga, Rev. Mod. Phys. **82**, 1225-1286 (2010).
- ³² D. R. Hofstadter, Phys. Rev. B **14**, 2239 (1976).
- ³³ H. Doh and S.-H. Suck Salk, Phys. Rev. B **57**, 1312 (1998).
- ³⁴ We note that the mathematical formulation of the current problem reduces to the Harper-Hofstadter model when $U = 0$, however the general problem with many-body interactions included can not be mapped to the 2D interacting Hofstadter problem as considered in Ref.³³. See the appendix for details.
- ³⁵ S. Chen, J. P. Cao and S. J. Gu, Phys. Rev. A **82**, 053625 (2010); EPL **85**, 60004 (2010).
- ³⁶ M. D. Girardeau and A. Minguzzi, Phys. Rev. Lett. **99**, 230402 (2007).
- ³⁷ L. Guan, S. Chen, Y. Wang, and Z. Q. Ma, Phys. Rev. Lett. **102**, 160402 (2009).
- ³⁸ G. Zürn, F. Serwane, T. Lompe, A. N. Wenz, M. G. Ries, J. E. Bohn, and S. Jochim, Phys. Rev. Lett. **108**, 075303 (2012).
- ³⁹ F. Deuretzbacher, *et al.*, Phys. Rev. Lett. **100**, 160405 (2008).
- ⁴⁰ D. J. Thouless, M. Kohmoto, M. P. Nightingale, and M. den Nijs, Phys. Rev. Lett. **49**, 405 (1982); M. Kohmoto, Annals of Physics **160**, 343 (1985).
- ⁴¹ Q. Niu, D. J. Thouless, and Y. S. Wu, Phys. Rev. B **31**, 3372 (1985).
- ⁴² E. H. Lieb and F. Y. Wu, Phys. Rev. Lett., **20**, 1445 (1968).
- ⁴³ For the superlattice system with $\alpha = 1/q$ under OBC, we note that behaviors of edge modes for the system with size of $L + q$ are almost the same as that of the system with size of L .
- ⁴⁴ P. Streda, J. Phys. C **15**, L717 (1982).
- ⁴⁵ E. Zhao, N. Bray-Ali, C. J. Williams, I. B. Spielman, and I. I. Satija, Phys. Rev. A **84**, 063629 (2011).
- ⁴⁶ L. Wang, A. A. Soluyanov, M. Troyer, Phys. Rev. Lett. **110**, 166802 (2013).